AMERICAN SOCIETY FOR MICROBIOLOGY | Applied and Environmental Microbiology®

BIOTECHNOLOGY

High-Density Cultivation of Terrestrial *Nostoc* Strains Leads to Reprogramming of Secondary Metabolome

Arthur Guljamow,[a] Marco Kreische,[a] Keishi Ishida,[b] Anton Liaimer,[c] Bjørn Altermark,[d] Lars Bähr,[e] Christian Hertweck,[b,f] Rudolf Ehwald,[e] Elke Dittmann[a]

University of Potsdam, Institute for Biochemistry and Biology, Potsdam-Golm, Germany[a]; Leibniz Institute for Natural Product Research and Infection Biology, Hans Knöll Institute, Jena, Germany[b]; Molecular Environments Group, Department of Arctic and Marine Biology, Faculty of Biosciences, Fisheries and Economics, University of Tromsø, Tromsø, Norway[c]; Department of Chemistry, Faculty of Science and Technology, University of Tromsø, Tromsø, Norway[d]; CellDEG GmbH, Berlin, Germany[e]; Natural Product Chemistry, Friedrich Schiller University, Jena, Germany[f]

ABSTRACT Terrestrial symbiotic cyanobacteria of the genus *Nostoc* exhibit a large potential for the production of bioactive natural products of the nonribosomal peptide, polyketide, and ribosomal peptide classes, and yet most of the biosynthetic gene clusters are silent under conventional cultivation conditions. In the present study, we utilized a high-density cultivation approach recently developed for phototrophic bacteria to rapidly generate biomass of the filamentous bacteria up to a density of 400 g (wet weight)/liter. Unexpectedly, integrated transcriptional and metabolomics studies uncovered a major reprogramming of the secondary metabolome of two *Nostoc* strains at high culture density and a governing effect of extracellular signals in this process. The holistic approach enabled capturing and structural elucidation of novel variants of anabaenopeptin, including one congener with potent allelopathic activity against a strain isolated from the same habitat. The study provides a snapshot on the role of cell-type-specific expression for the formation of natural products in cyanobacteria.

IMPORTANCE Terrestrial filamentous cyanobacteria are a largely untapped source of small-molecule natural products. Exploitation of the phototrophic organisms is hampered by their slow growth and the requirement of photobioreactors. The present study not only demonstrates the suitability of a recently developed two-tier vessel cultivation approach for the rapid generation of biomass of *Nostoc* strains but also demonstrates a pronounced upregulation of high value natural products at ultrahigh culture densities. The study provides new guidelines for high-throughput screening and exploitation of small-molecule natural products and can facilitate the discovery new bioactive products from terrestrial cyanobacteria.

KEYWORDS allelopathy, cellular differentiation, cyanobacteria, natural products, nonribosomal peptide

Cyanobacteria are one of the most prolific sources of small-molecule natural products featuring potent bioactivities, as well as exhibiting unique structural properties (1–3). Phylogenomic surveys of cyanobacteria have revealed a large number of orphan biosynthetic gene clusters (BGCs) that await mining and characterization of their products, in particular in late-branching lineages of the cyanobacterial phylum (4, 5). Traditional bioactivity-guided screening techniques have uncovered a distinct metabolic profile of strains from freshwater, marine, and terrestrial habitats (6, 7). However, structural and functional characterization of the actual compounds is strongly biased

Received 10 July 2017 **Accepted** 18 September 2017

Accepted manuscript posted online 22 September 2017

Citation Guljamow A, Kreische M, Ishida K, Liaimer A, Altermark B, Bähr L, Hertweck C, Ehwald R, Dittmann E. 2017. High-density cultivation of terrestrial *Nostoc* strains leads to reprogramming of secondary metabolome. Appl Environ Microbiol 83:e01510-17. https://doi.org/10.1128/AEM.01510-17.

Editor Claire Vieille, Michigan State University

Address correspondence to Elke Dittmann, editt@uni-potsdam.de.

A.G. and M.K. contributed equally to this article.

toward strains from freshwater and marine habitats that are known as producers of notorious toxins (4). Although the biosynthetic potential of terrestrial strains has been recognized (8), attempts to assess the full biosynthetic capacity of these slow growing organisms are often hampered by the requirement of larger amounts of biomass.

Two major problems complicate high-density (HD) cultivation of cyanobacteria: light attenuation in dense cultures that strongly limits the available light for net photosynthesis and an insufficient supply of inorganic carbon (9). Although the first problem was successfully addressed in flat-plate bioreactors with rapid turbulent mixing, media buffered with saturating concentrations of HCO_3 pose a considerable risk of developing a high pH as a result of photosynthesis that, in turn, can ultimately lead to chronic photoinhibition. Ehwald and coworkers recently developed a two-tier vessel for photoautotrophic growth in which a cyanobacterial culture and a high-CO_2 buffer are shaken in two distinct compartments that are separated by a gas-permeable polypropylene membrane (9). The device enabled rapid growth of the unicellular model cyanobacteria *Synechocystis* sp. strain PCC 6803 and *Synechococcus* sp. to ultrahigh densities of up to 30 g (dry weight) liter^{-1}.

Here, we evaluated whether the same approach is suitable for the high-density cultivation of the filamentous terrestrial cyanobacterium *Nostoc*. Strains of this genus are extremely versatile and are found both in a free-living state and in symbiosis with plants from diverse taxa. Remarkably, *Nostoc* spp. feature one of the most sophisticated life cycles in the microbial world. Individual strains are capable of differentiating distinct cell and filament types, namely, vegetative cells, nitrogen-fixing heterocysts, spore-like akinetes, and motile hormogonia (10). The genome of the model strain *Nostoc punctiforme* PCC 73102 harbors a large number of BGCs encoding nonribosomal peptide synthetases (NRPS) and polyketide synthases (PKS), as well as ribosomal natural product pathways (RiPPs). While at least two of the corresponding metabolites, nostopeptolide and the cryptic product of the *pks2* pathway, have been linked to cellular differentiation recently (11, 12), less is known about the impact of cell density on secondary metabolite production. Uncovering a potential connection is of considerable relevance, since cell density is a critical factor for secondary metabolite production in a large number of heterotrophic bacteria, including *Streptomycetes*, well known producers of potent antibiotics (13). Production of high-value natural products in these organisms is controlled by quorum-sensing signals such as gamma-butyrolactone (13). As a consequence, complex secondary metabolites mostly accumulate in the stationary phase. Although common quorum-sensing signal molecules of the N-acyl homoserine lactone type were incidentally reported for cyanobacteria and were shown to trigger a specific signaling response in the strain *Gloeothece* sp. strain PCC 6909 (14), the responsible biosynthetic protein LuxI is not encoded in the majority of cyanobacterial genomes. While a recent study has reported cell density effects on the accumulation of the potent cyanotoxin microcystin (15), most authors have reported a rather constitutive production of the toxin concomitant to growth from the initial logarithmic phase onward, arguing against a major control by cell-density-dependent factors (16).

The present study aims to assess the suitability of the two-tier high-density cultivation for the rapid production of biomass of *Nostoc punctiforme* and to systematically analyze the impact of this form of cultivation on secondary metabolite production. This study not only provides fundamental insights into the role cell density and cell-type-specific expression play in the production of high-value secondary metabolites of *N. punctiforme* but also offers guidelines for further exploitation of natural products of terrestrial *Nostoc* strains, as well as for the optimization of screening protocols.

RESULTS

Growth of *N. punctiforme* in two-tier vessels. Cultivation of the strain *N. punctiforme* PCC 73102 in shaken two-tier vessels enabled rapid growth of the cyanobacteria up to a cell density of 380 g (wet weight)/liter (Fig. 1). Biomass continued to increase over a period of 20 days. Parallel-grown conventional (C) batch cultures without additional CO_2 supply reached only 15 g (wet weight) in the same time period, though

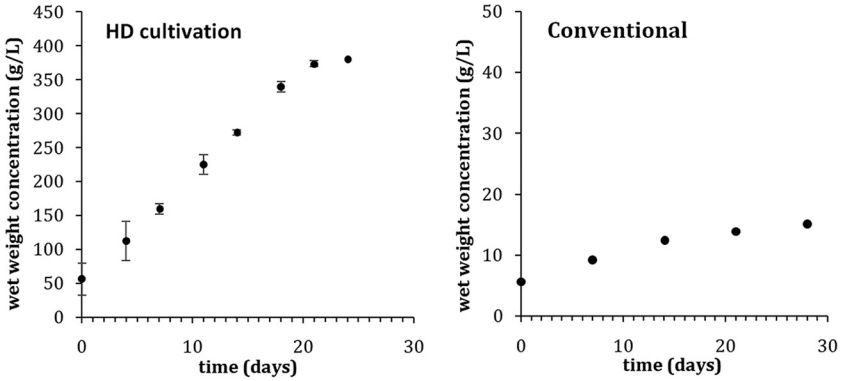

FIG 1 (Left) Growth curve of a high-density (HD) culture of *N. punctiforme* PCC 73102. (Right) Growth curve of a conventional (C) culture of *N. punctiforme* PCC 73102, grown without an additional CO_2 supply. The means of two biological replicates are shown.

a larger inoculum was utilized for HD cultivation (Fig. 1). Specific growth rates in the HD culture during exponential growth clearly exceeded the growth rate in the C culture. In the HD vessels, *N. punctiforme* grew in the form of dense tufts, while *N. punctiforme* filaments in the C culture formed more loosely associated clusters (Fig. 2). Vegetative filaments were predominant in both cultivation types (Fig. 2).

Transcriptional analysis of BGCs reveals reprogramming of secondary metabolome. The biomass of *N. punctiforme* PCC 73102 was harvested after 24 days of HD and C cultivation, respectively, and subjected to RNA isolation and transcriptional analysis of BGCs. *In silico* analysis of the resequenced genome of *N. punctiforme* PCC 73102 using the AntiSMASH platform (17) revealed 14 BGCs of the NRPS, PKS, and RiPP types, including two that were recently assigned to the bioactive metabolites, nostopeptolide and anabaenopeptin (Table 1). For each of these BGCs, reverse transcription-PCR (RT-PCR) primers were designed for a core biosynthetic gene (Tables 1 and 2). Two primer pairs were designed for one of the RiPP clusters (ripp1 in Table 1), since the BGC boundaries were not clearly traceable, increasing the overall number of BGC genes analyzed to 15. Each BGC was connected to the cluster identifier generated by the AntiSMASH platform (Table 1). The transcription of each BGC was normalized to the *rnpB* housekeeping gene. Comparison of the transcriptional levels of HD cultivation versus C cultivation revealed a strong transcriptional reprogramming of BGCs (Fig. 3A). Transcripts of three of the BGCs were accumulating in significantly larger amounts in HD cultures (ratio HD versus C culture $>$ 2), with two of the cryptic PKS gene clusters reaching factors of 10 and 7, respectively (BGCs 3 and 9). The recently described anabaenopeptin BGC showed a 3-fold increase in transcript levels (BGC 5). For five BGCs, on the other hand, the transcript levels in the C culture were up to 3-fold higher, including two orphan PKS and NRPS gene clusters (BGCs 20 and pC1). Transcription of the nostopeptolide BGC (BGC 4) and seven further BGCs was almost unchanged.

HPLC analysis of *N. punctiforme* extracts and supernatants. In parallel to the transcriptional analysis, equal amounts of biomass from the two cultivation approaches were extracted and analyzed by high-performance liquid chromatography (HPLC) and matrix-assisted laser desorption ionization–time of flight (MALDI-TOF) mass spectrometry (MS) analysis. Supernatants of the cultures were analyzed concomitantly. Two peaks could be assigned to nostopeptolide 1052 (peak 1, *m/z* 1,052) and nostopeptolide A (peak 2, *m/z* 1,081), based on comparison with standards and MALDI-TOF MS (Fig. 3B and see Fig. S1 in the supplemental material). Several smaller peaks were increased in the HD pellet (peaks 3 to 5), the largest of which could be assigned to nostamide A (peak 3, see Fig. S1 in the supplemental material). The anabaenopeptin variant was previously reported for strain PCC 73102, albeit in trace amounts (18). The identity of the three compounds was further confirmed using MALDI-TOF MS post-source decay (PSD) fragmentation (see Tables S5 and S6 and Fig. S2 and S3 in the

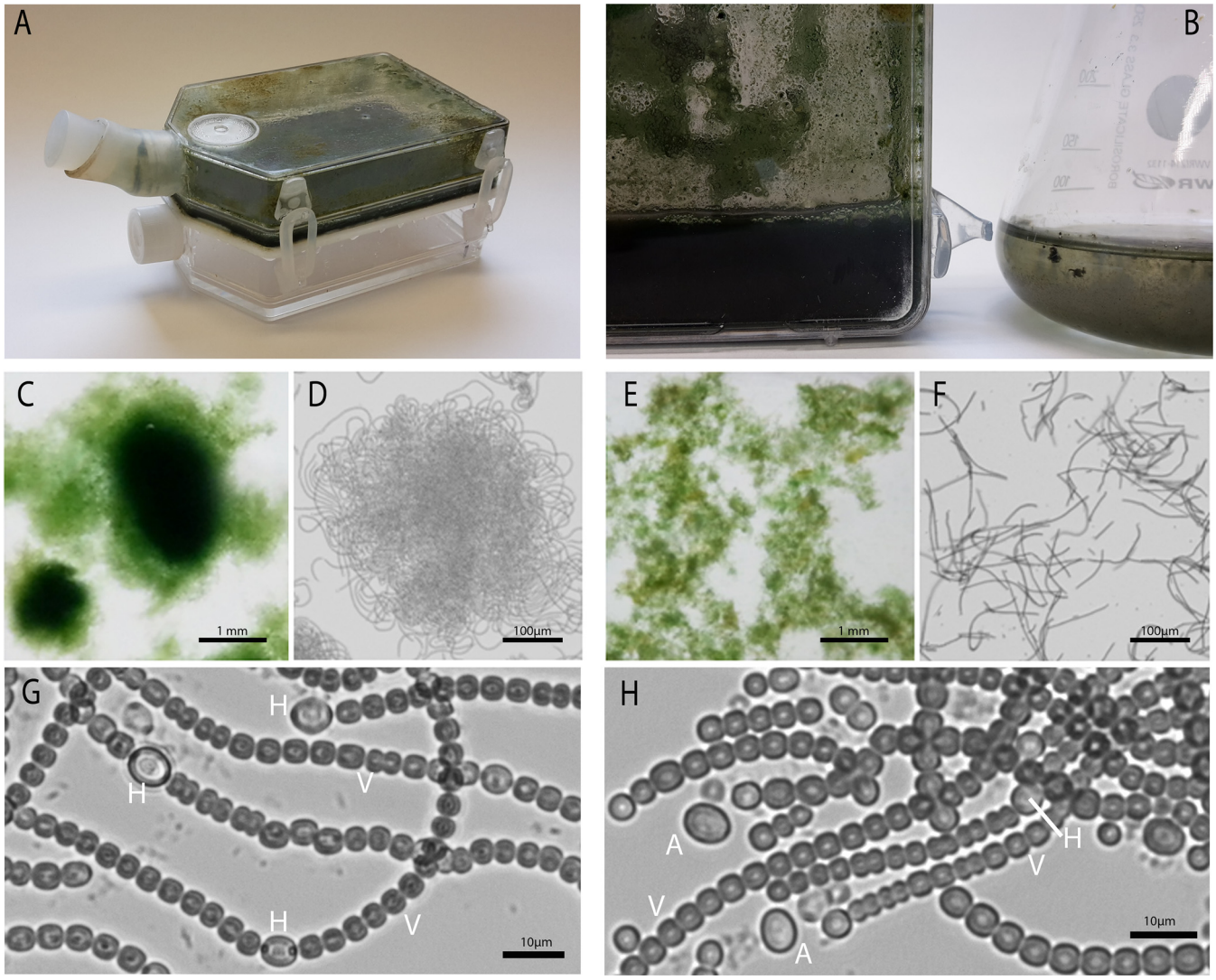

FIG 2 Macroscopic and microscopic appearances of *N. punctiforme* PCC 73102 in HD and C batch cultures. (A) Two-tier growth vessel with thick biofilm of *N. punctiforme.* (B) Comparison of cell densities in HD (left) and C (right) cultivation. (C) Tufts of *N. punctiforme* observed in HD cultures. (D) Microscopic overview of *N. punctiforme* filament aggregation in HD cultures. (E) Cluster of filaments of *N. punctiforme* observed in C cultures. (F) Loose packing of filaments of *N. punctiforme* in C cultures. (G and H) Cell types observed in HD and C cultures, respectively. Labels: V, vegetative cell; H, heterocyst; A, enlarged single cell.

supplemental material). The larger amount of anabaenopeptin is in agreement with the increased transcription of the corresponding BGC 5 in HD cultures. Supernatants of the two cultures revealed a strong increase of three major peaks in the HD cultures. Two of these peaks could be assigned to nostopeptolide A and nostamide A (peaks 1 and 3), while the third peak (peak 6) did not yield a clear ionization spectrum using MALDI-TOF MS (see Fig. S1 in the supplemental material). Taken together, HD cultivation led to the upregulation of nostamide A and several other not-yet-identified metabolites in *N. punctiforme* PCC 73102.

Reprogramming of secondary metabolomes after medium exchange. C cultivation and HD cultivation differ in a number of aspects, including light conditions, CO_2 supply, shaking conditions, and medium volume. In order to estimate how much the enrichment of medium factors contributes to the reprogramming of the secondary metabolome, we included a third cultivation approach in which we supplied the supernatant of the HD culture to a duplicate of the C culture for the last 7 days of cultivation. For that purpose, HD supernatant was collected at day 17 of HD cultivation. HPLC analysis of the supernatant revealed a close similarity to the HD supernatant after

TABLE 1 BGCs of *N. punctiforme* PCC 73102 analyzed in this study

Cluster no.[a]	Name[b]	Gene identifier[c]	Cluster position	
			Start	End
3	pks1	Npun_R2072-Npun_R2091	2503324	2568631
4	Nos	Npun_R2174-Npun_F2190	2633241	2723454
5	Apt	Npun_F2459-Npun_F2465	3035744	3097661
8	nrps1	Npun_R3022-Npun_F3034	3699016	3800010
9	pks2	Npun_R3153-Npun_R3179	3881285	3975345
10	ripp1	Npun_F3202-Npun_F3235	3983720	4027282
11	ripp2	Npun_R3312-Npun_R3313	4108476	4132422
12	pks3	Npun_R3353-Npun_F3370	4166429	4220200
13a	ripp3	Npun_R3388-Npun_R3395	4233288	4243620
13b	pks4	Npun_F3414-Npun_R3453	4243100	4350413
15	ripp4	Npun_F5045-Npun_F5052	6245456	6264724
17	ripp5	Npun_F6115	7560732	7560965
20	pks5	Npun_R6584-Npun_R6592	8130738	8187006
pC1	nrps2	Npun_CR070-Npun_CR075	79346	106817

[a]That is, the cluster identifier BGC number according to AntiSMASH4.0.
[b]"Nos" and "Apt" denote the BGCs for nostopeptolide and anabaenopeptin, respectively. The cluster "nrps2" is encoded on one of the five plasmids of *N. punctiforme* PCC 73102.
[c]Database accession numbers according to CyanoBase (http://genome.microbedb.jp/cyanobase).

24 days of HD cultivation (Fig. 3 and see Fig. S4 in the supplemental material). The culture treated with the HD supernatant was harvested in parallel to the conventional culture after 24 days. Transcriptional analysis of the BGCs of this culture (C+HD medium) revealed an upregulation of all BGCs that were upregulated in the HD culture, although not always to the same extent (Fig. 4A). Neither removal and readdition of the supernatant of the conventional culture (C+C supernatant) nor continuous shaking of the culture had a similar effect on the metabolite spectrum in the cellular extract or supernatant thereby excluding a plain mechanical effect (see Fig. S5 in the supplemental material). These data clearly suggest that the upregulation of the BGCs in HD cultures is primarily due to medium factors. In addition, five further gene clusters were up to 8-fold upregulated. HPLC analysis revealed that two peaks were boosted in this cultivation approach that were only slightly increased in the HD cultivation (peaks 4 and 5) (Fig. 4B). MALDI-TOF MS analysis revealed masses (M+Na) of 2,140 for peak 4 and 2,168 for peak 5, respectively. The two peaks were accompanied by a third peak (peak 7) in the same mass range (M+Na, 2,197) (see Fig. S1 in the supplemental material). The assignment of the masses to specific BGCs is part of ongoing research.

TABLE 2 Biosynthetic gene clusters and primers used for the detection of their cDNA in rtPCR

Cluster no. (AntiSMASH)	Name[a]	Primer	Target gene		Primer sequence (5′–3′)		PCR product size (bp)
			CyanoBase[b]	AntiSMASH	Left	Right	
3	pks1	C3	R2082	10475	CGTGGTTGACTGGAGATGCT	AAGCCTCTCGTGCCGTTTTA	108
4	Nos	nosA_RT4	F2181	10970	GTTTGCCCTCTCTGCTGAAC	GCGGTAAAGCAGGGTATCAA	109
5	Apt	apt_RT	F2460	12350	GAAATTGAGGCGCTTTTGAG	GGCTAGTGACGCTCACATCA	136
8	nrps1	C8	R3027	15385	AGCGGCAACATATTCCCCAA	ACGCCCAACCTGCTCTATTC	113
9	pks2	C9	F3163	16005	AAATCTTCGCCAGCATCCCA	TTGGCAACCTCCCCTTGTAC	101
10	ripp1	C10r	F3226	16320	GCAACTCTATAGCGCTCAAGG	GCTGTCTCTCCTGCATGACA	107
		C10L	R3212	16255	GGCAGAATTGGGAGGACGAA	TCCCAAACCCATCATTGAGCA	111
11	ripp2	C11a	R3313	16795	AGCAGACATCATAGCTCCACT	GGGTGCAGAAAAGGGCTACA	130
12	pks3	C12	F3359	17020	AGCTTGATGTTGTCTCCGCA	CTTCACCACGGACGTAACCA	115
13a	ripp3	C13a	R3395	17180	GGGTGGCCATACAACTCCAT	ATCTGCCGATGGTGAAGGTG	118
13b	pks4	C13b	R3445	17420	GGTGCAACCCGAAATCACAC	CAATGCTGGCTGTTCCCCTA	110
15	ripp4	C15	F5047	25520	TGATGGGGAAGCAACAGGTG	GAGGCGTTCAAGTTCGATGC	128
17	ripp5	C17	F6115	31000	GAGCGTGGTTATGACTTCACA	GTGCCGTCTAGTTCCCCATC	108
20	pks5	C20	R6590	33540	GGGGAATGGAAAGCATGGGA	ATTAACGCCCCTTCCCTGTG	125
pC1	nrps2	Cp	CR074	CR074	CTCATGTCGGGTGCAGCTTA	CCTCAATCCAAGTCAGGCGT	136
		rnpB_RT3	R018		GCGGTTGCAGATCAGTCATA	TCTGTGGCACTATCCTCACG	110

[a]As previously reported by Liaimer et al. (12).
[b]Database accession numbers according to CyanoBase (http://genome.microbedb.jp/cyanobase).

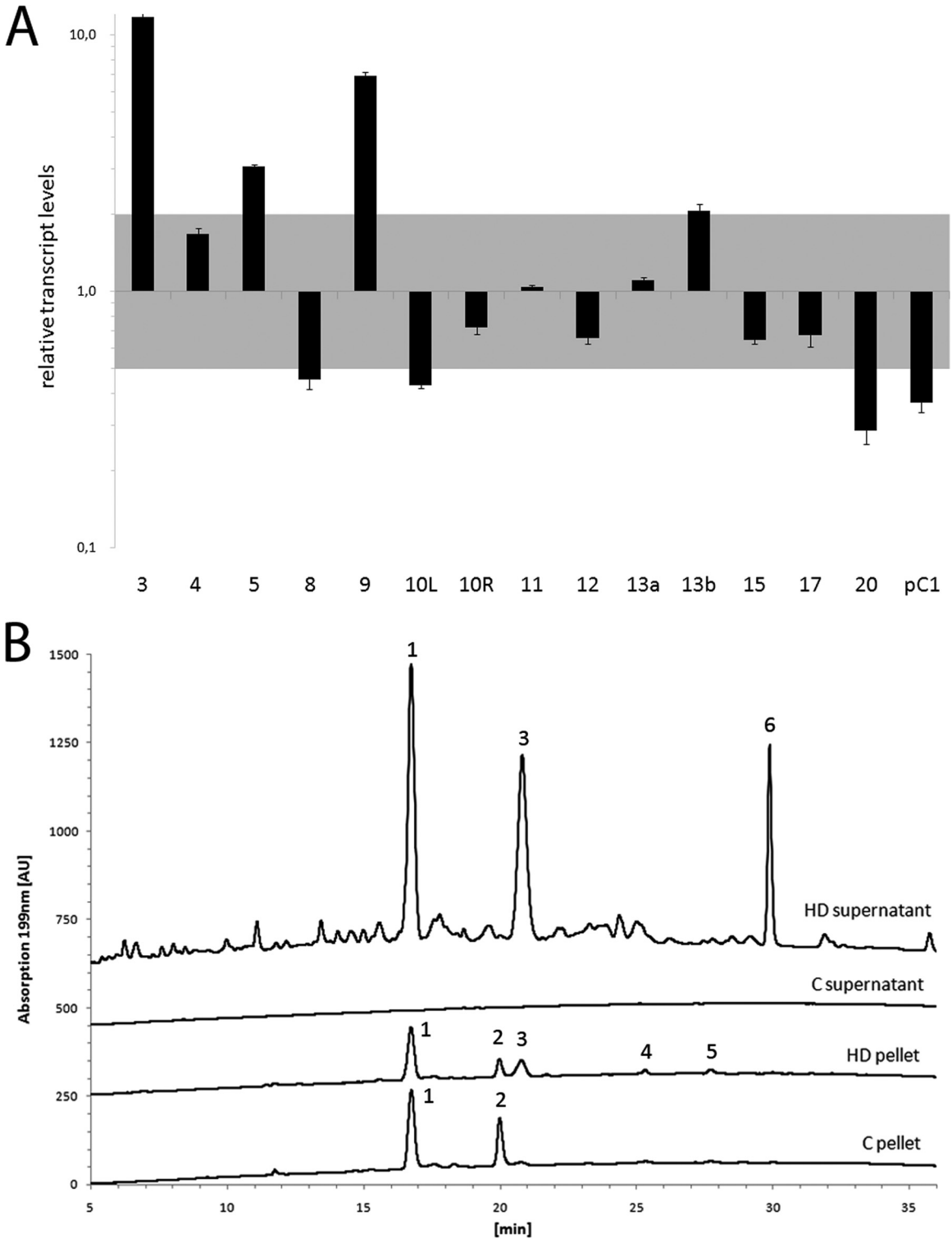

FIG 3 Comparison of BGC transcription and metabolite accumulation in HD and C cultivation. (A) Relative transcription of BGCs in HD versus C cultivation. All transcript levels were normalized to the *rnpB* housekeeping gene. Numbers relate to the BGC identifiers of the AntiSMASH platform as listed in Table 1 The relative transcript level range between −0.5 and 2 is shaded in gray. (B) HPLC profiles of cellular extracts and supernatants of *N. punctiforme* PCC 73102 from HD and C cultures. The results of MALDI-TOF analysis of the peaks 1 to 6 are shown in Fig. S1 in the supplemental material. Peaks: 1, nostopeptolide 1052; 2, nostopeptolide A; 3, nostamide A; 4 to 6, unknown. AU, absorbance units.

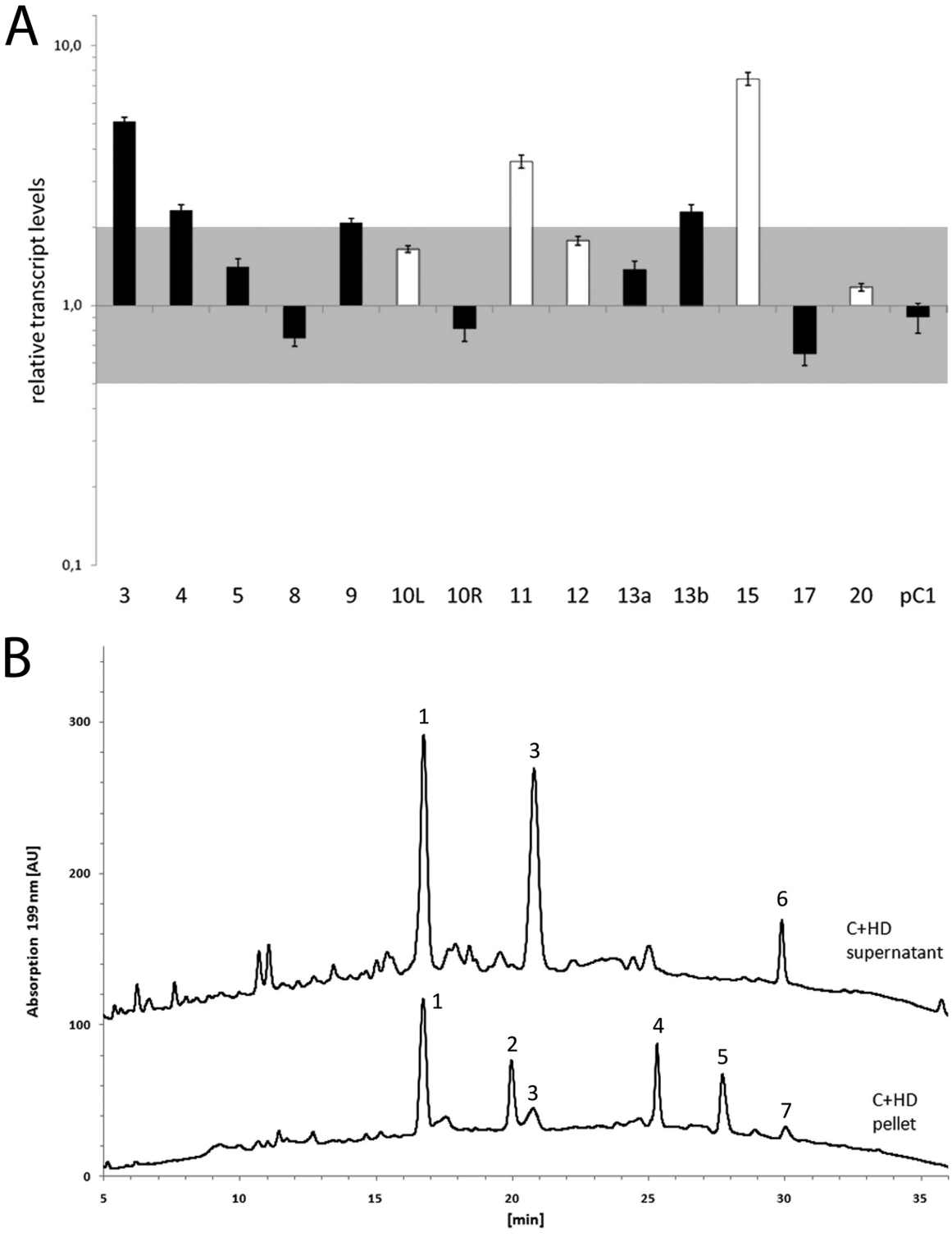

FIG 4 Comparison of BGC transcription and metabolite accumulation in a C culture treated with HD supernatant for 7 days (C+HD) and C cultivation. (A) Relative transcription of BGCs in C+HD versus C cultivation. All transcript levels were normalized to the *rnpB* housekeeping gene. The relative transcript level range between −0.5 and 2 is shaded in gray. Numbers relate to the BGC identifiers of the AntiSMASH platform, as listed in Table 1. White bars highlight BGCs that are exclusively upregulated in C+HD cultures. (B) HPLC profile of cellular extracts and supernatants of *N. punctiforme* PCC 73102 from C+HD cultures. The results of MALDI-TOF analysis of peaks 1 to 7 are given in Fig. S1 in the supplemental material; the results of MALDI-TOF MS PSD analysis of peaks 1 to 3 are given in Fig. S2 in the supplemental material. The HPLC profiles of conventional cultures grown without treatment are shown in Fig. 3. Peaks: 1, nostopeptolide 1052; 2, nostopeptolide A; 3, nostamide A; 4 to 7, unknown.

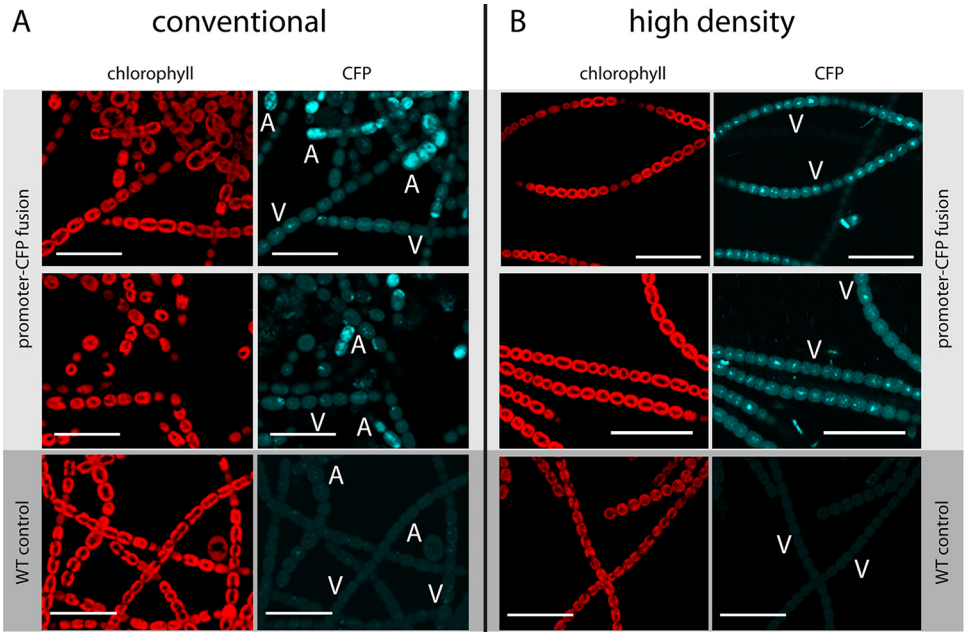

FIG 5 Fluorescence micrographs of an p_{Apt}-CFP transcriptional reporter of *N. punctiforme* PCC 73102 grown under C conditions (A) or HD conditions (B). Although CFP fluorescence (right column) in conventional culturing is restricted to enlarged akinete like cells (labeled "A"), CFP fluorescence in HD cultures is prevalent in vegetative filaments (labeled "V"). Red chlorophyll autofluorescence (left column) is shown to visualize intact cells. Two biological replicates are shown. Scale bar, 20 μm.

Analysis of a transcriptional reporter of the anabaenopeptin BGC. In order to analyze whether the HD cultivation approach has an impact on cell-type-specific expression in *N. punctiforme*, the 374-bp 5′ untranslated region (UTR) of the anabaenopeptin biosynthesis gene *aptA* was fused to the cyan fluorescence protein (CFP) gene and expressed from an autonomously replicating plasmid (P-aptA-CFP). In conventional cultures, a bright fluorescence was visible for discrete cells within vegetative filaments and single cells. Fluorescent cells were typically larger than vegetative cells supporting an expression of anabaenopeptin in the (pre-)akinete state (Fig. 5). The small amount of these types of cells observed in conventional cultures explains the trace amount of anabaenopeptins that are typically detectable under these growth conditions. Filaments from the HD cultivation exhibited a rather even fluorescence within cells of longer vegetative filaments, suggesting that HD cultivation diminishes the spatial restriction of the anabaenopeptin BGC transcription (Fig. 5). Hence, the larger amount of anabaenopeptin is not due to an increase of *apt* transcription in individual cells but rather due to transcription by an overall larger number of vegetative cells.

Utilization of the HD cultivation approach for the genomic mining of novel anabaenopeptins. The HD cultivation approach was further tested with *Nostoc* sp. strain KVJ2 that was recently isolated from *Blasia pusilla* in Northern Norway and is phylogenetically distant from *N. punctiforme* PCC 73102 (19). The strain reached a cell density similar to that reached by strain PCC 73102 (400 g [wet weight]/liter) in a period of 20 days (Fig. 6A). Comparison of the metabolite profiles of the KVJ2 strain extracted after HD cultivation with a conventional culture grown in parallel showed pronounced differences between the two cultivation conditions (Fig. 6B). Three of the major peaks strongly upregulated under HD conditions were identified as anabaenopeptins (Fig. 6B). Notably, anabaenopeptins were not detected in a recent study in which strain KVJ2 was reported to produce only aeruginosin and nostocyclopeptide (19). Indeed, in conventional cultures, anabaenopeptins are virtually absent in extracts of that strain (Fig. 6B). The analysis of a draft genome of KVJ2 revealed the presence of an anabaenopeptin gene cluster that closely resembles the cluster of *N. punctiforme* PCC 73102 in the composition of domains within the NRPS AptA-D (18). For one of the

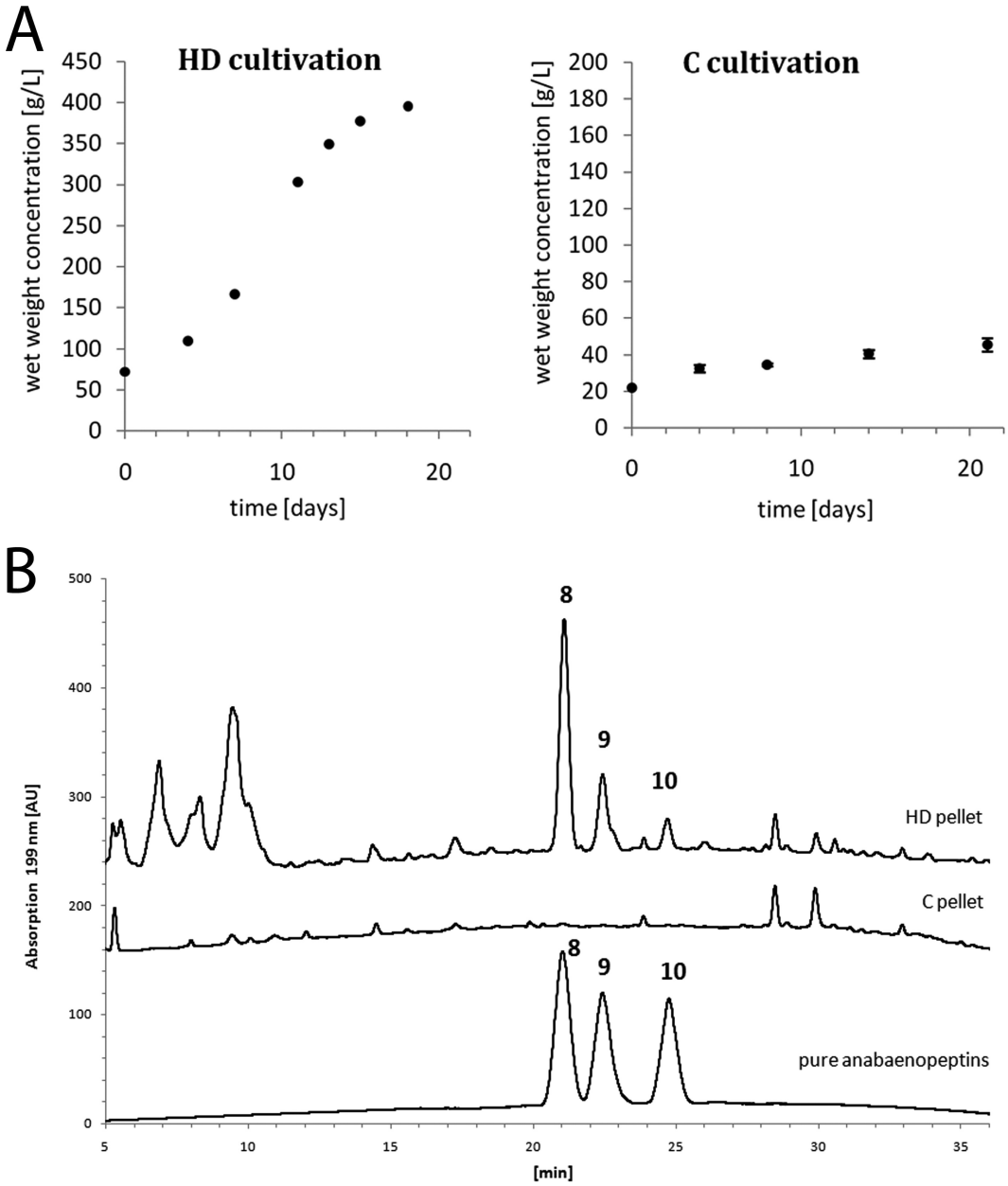

FIG 6 (A) Growth curves of KVJ2 from an HD culture (left) and a C culture (right). (B) HPLC profiles of KVJ2 cellular pellet extracts from HD and C cultures. A profile of three anabaenopeptins purified from KVJ2 is shown for comparison. Peaks: 8, anabaenopeptin KVJ827; 9, anabaenopeptin KVJ841; 10, anabaenopeptin KVJ811.

adenylation domains, a divergent amino acid specificity was predicted using the software NRPSpredictor2 compared to the *apt* gene cluster of PCC 73102: Tyr instead of Phe for AptA1 (Fig. 7A) (18). Three anabaenopeptins were purified by reversed-phase HPLC. Nuclear magnetic resonance (NMR) spectral analysis was only carried out for anabaenopeptin 8 isolated as a main metabolite (Fig. 7B; see also Fig. S6 to S11 and Table S3 in the supplemental material). The structures of two other congeners, congeners 9 and 10, were deduced by MALDI TOF MS PSD analysis (see Table S6 and Fig. S12 in the supplemental material). The stereochemistry of these peptides was elucidated by the HPLC analysis of FDAA [N^{α}-(5-fluoro-2,4-dinitrophenyl)-L-alaninamide] derivatives (see Fig. S13 to S17 in the supplemental material). The structures of the new anabaenopeptins KVJ827, KVJ841, and KVJ811 are very similar to those of anabaenopeptin congeners from *Anabaena* sp. TAU strain NZ-3-1 and *N. punctiforme* PCC 73102 (see

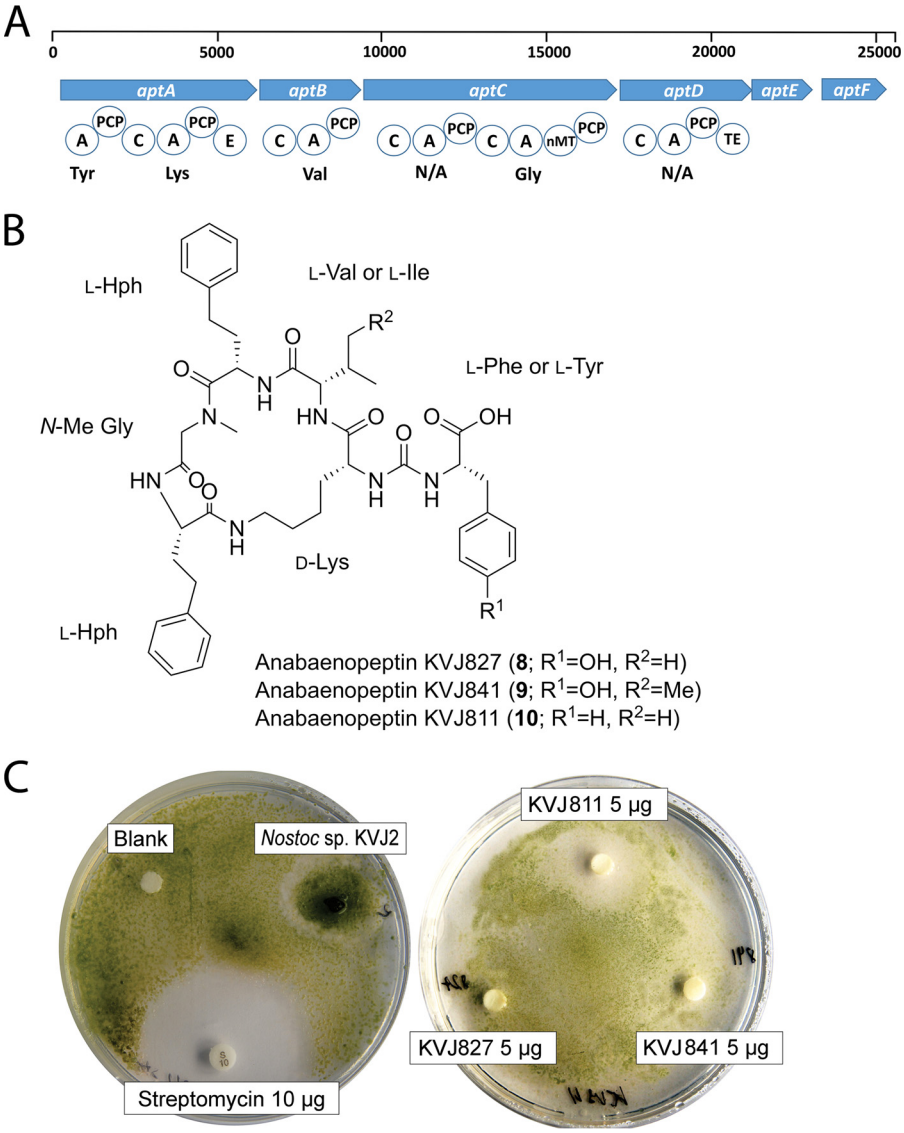

FIG 7 Anabaenopeptins detected in *Nostoc* sp. strain KVJ2. (A) Schematic representation of the anabaenopeptin gene cluster of strain KVJ2. The domain composition of the encoded NRPS assembly line is shown below the genes. Abbreviations: A, adenylation domain; PCP, peptidyl carrier protein; C, condensation domain; E, epimerization domain; TE, thioesterase. The amino acid specificities of the adenylation domain, as predicted by NRPSpredictor2 (32), are indicated. (B) Structures of anabaenopeptins KVJ827, KVJ841, and KVJ811 detected during this study. (C) Results from an allelopathy test of novel anabaenopeptins against strain KVJ11 isolated from the same habitat. (Left) controls; (right) 5 μg of anabaenopeptin KVJ827, KVJ811, and KVJ841, as indicated.

Table S3 in the supplemental material) (18, 20). As Carmeli and coworkers argued, anabaenopeptins possessing *N*-methyl glycine have two conformational isomers due to the presence of two energetically equal rotamers of *N*-methyl glycine. Hence, anabaenopeptin KVJ827 also showed two sets of chemical shifts for two conformers (see Fig. S15 in the supplemental material). Corresponding to the altered amino acid specificity predicted for AptA1, two of the anabaenopeptins contained Tyr instead of Phe in position 1 (see Table S2 in the supplemental material). Since *Nostoc* sp. strain KVJ2 exhibited allelopathic activities against other *Nostoc* strains from the same habitat in a recent study (19), 5 μg of each anabaenopeptin variant was tested in an allelopathy assay with the sensitive strain *Nostoc* sp. KVS11. Remarkably, anabaenopeptin KVJ811, but not the major variant KVJ827, triggered pronounced allelopathic effects against strain KVJ827 (Fig. 7C). The paper discs containing KVJ811 showed well-defined inhi-

bition zones reaching 23.33 ± 3.05 mm in diameter. For comparison, the colonies of the tester strain *Nostoc* sp. KVJ2 exhibited inhibition zones that were 1.2 to 1.4 times larger than the colony diameter.

DISCUSSION

Despite its recognized biosynthetic potential, exploitation of cyanobacterial natural products is still in its infancy (1, 3, 8). The largest challenge for an extensive utilization of terrestrial cyanobacteria as a source of novel natural products is the production of sufficient amounts of biomass from these slow-growing organisms. The present study demonstrates that the recently developed technique of culturing photoautotrophic microorganisms with ultrahigh cell density by shaking on CO_2-saturated porous hydrophobic membranes (9) not only enables rapid cultivation of filamentous cyanobacteria for the production of high-value natural products but also suggests that HD cultivation can aid in mining parts of the large hidden natural product diversity of the genus *Nostoc*.

Small-molecule natural products confer adaptive advantages to the producing organisms and correlate with the complexity of the ecological niche in which the organisms grow. Hence, the benefit of a given metabolite may only be relevant in the context of a specific habitat (21, 22). In the field, terrestrial strains of the genus *Nostoc* often grow as dense colonies of filaments in a gelatinous matrix frequently reaching macroscopically visible dimensions (23). Signaling within these biofilms relies on diffusion properties in soil and the extracellular matrix that are fundamentally different from marine or freshwater habitats. The rather low turbulent flow in the HD cultivation device and the formation of dense tufts of filaments may thus more closely resemble the growth of terrestrial *Nostoc* bacteria in their natural habitat.

Differences in small-molecule natural product accumulation during HD cultivation were most pronounced in the supernatant of the culture. However, increased accumulation of compounds was highly specific, e.g., only one of two major nostopeptolide variants found in the pellet fraction was detected in the supernatant. It was the supernatant, again, that triggered an upregulation of a considerable number of BGCs in the conventional culture. These data clearly demonstrate that extracellular signaling is a major trigger of BGC expression in terrestrial *Nostoc* strains. The fact that more BGCs were upregulated when the HD supernatant was added to the C culture than in the HD culture itself may indicate that the immediate response to metabolites accumulating in the medium is more pronounced than after continuous cultivation at high density. Simultaneous upregulation of a large number of BGCs may constitute a large metabolic burden for the cells that could be counterbalanced by feedback regulation mechanisms. Notably, three of the metabolites weakly upregulated in HD culture (peaks 4, 5, and 7) were strongly upregulated in the C+HD substitution experiment. This phenomenon could be explained by an autoinduction of the corresponding genes. The governing role of extracellular signals produced at high density on BGC transcription in low-density cultures indicates the existence of a quorum-sensing-like mechanism(s) in *N. punctiforme* PCC 73102. The nature of the signal(s) and the regulatory network have yet to be identified.

Anabaenopeptins were selected to demonstrate the power of the HD cultivation approach to facilitate structural characterization of new natural products. Anabaenopeptins are a highly diverse family of cyclic heptapeptides characterized by an ureido-linkage connecting the side chain amino acids to D-lysine. Members of this family are potent protease inhibitors and have served as lead products for the design of inhibitors against carboxypeptidase TAFIa (24). Although anabaenopeptin production has been principally demonstrated for *N. punctiforme* PCC 73102, no larger amount could be obtained for further characterization (18). Since the identity of the corresponding BGC is known, production of the compound could clearly be correlated with transcription by both RT-PCR and a fluorescence reporter strain. The well-known tandem MS (MS/MS) fragment spectrum of anabaenopeptins enabled the easy detection of the compounds. The metabolite was thus considered a suitable candidate to demonstrate that the

increased accumulation of transcripts is indeed reflected at the metabolite level. Anabaenopeptin could not only be identified in much larger amounts in HD extracts of *N. punctiforme* PCC 73102 but also in the strain KVJ2 that was recently isolated from *Blasia pusilla* in Northern Norway (19). In both strains, anabaenopeptin production was very low or absent in conventional cultivations, whereas major peaks were detected in HD cultures. As part of this study, we could demonstrate an allelopathic activity against another *Nostoc* strain for one of the anabaenopeptin variants. These findings support a role of anabaenopeptins in the anticyanobacterial effects observed for strain KVJ2 in a recent study (19). Anabaenopeptins were recently reported to trigger allelopathic effects in cyanobacterial strains of the genus *Microcystis* (25). The fact that only one of the three closely related anabaenopeptin congeners tested showed this activity is striking and suggests that the ongoing diversification of anabaenopeptins might be driven by intraspecific interactions between *Nostoc* strains. Analysis of the promoter-CFP reporter fusion construct revealed that transcription of anabaenopeptin biosynthesis genes is limited to a few cells in C cultures, whereas it is clearly extended in HD cultures. Although the expression seemed rather cell type specific in C cultures and was apparently connected to early akinetes, the cell-specific restriction was abrogated in HD cultures. These data further strengthen the hypothesis that secondary metabolites are connected to cellular differentiation of *N. punctiforme* (11), although the specific role of anabaenopeptin in this network and the mechanistic basis underlying the expression pattern are currently unknown.

Considering the large number of BGCs differentially regulated and the pronounced differences in the HPLC profiles, anabaenopeptins likely represent only the tip of an iceberg. The present study can be used as a template for the discovery and structural elucidation of entirely new types of compounds. Moreover, it proves the suitability of the HD cultivation approach for filamentous cyanobacteria of the genus *Nostoc* and demonstrates the accelerated generation of biomass. Clearly, the reprogramming of the secondary metabolomes in HD cultivation can guide further exploitation of terrestrial strains of the genus *Nostoc* and should be considered in high-throughput screening protocols.

MATERIALS AND METHODS

Cultivation of cyanobacteria. *Nostoc* was grown in liquid culture at a constant temperature of 21°C under continuous light and diazotrophic conditions in $BG11_0$ growth medium (26). *N. punctiforme* PCC 73102 was obtained from the Pasteur Culture Collection of Cyanobacteria (PCC). *Nostoc* sp. strain KVJ2 was recently isolated from *B. pusilla* in Northern Norway (19). For conventional cultivation, cells were grown in 100-ml Erlenmeyer flasks with a final volume of 25 ml under white light at an intensity of 30 μmol photons/m^{2}s without shaking. For high-density cultivation, a two-tier vessel system was used (9). Essentially, cells in a liquid culture chamber were connected through a highly gas-permeable polypropylene membrane with a second chamber containing a bicarbonate buffer that maintains a high CO_2 concentration in the gas atmosphere within the membrane pores. The high shear velocity in the shaken growth medium above the membrane brings about rapid CO_2 dissolution and thus prevents carbon deficiency in dense cultures with high volumetric assimilation rates. An O_2 outlet channel with suitable dimensions prevented both significant oxygen accumulation within the culture of photosynthesizing cyanobacteria and strong release of water vapor from the culture. Both the culture vessel and the buffer vessel applied in this study had a total capacity of 900 ml, and the volumes of both buffer and liquid growth medium were 100 ml. Carbonate buffer was obtained by combining solutions of 3 M $KHCO_3$ and 3 M K_2CO_3 at ratios of 4:1 or 9:1, yielding CO_2 partial pressures of 3,200 and 9,000 Pa, respectively. Cells were illuminated with a HYG05-D100*3W-W full-spectrum LED panel and shaken at ca. 200 rpm. Carbonate buffer concentration and light intensity were adjusted to cell density (see Table S1 in the supplemental material). The whole culture was spun down (3,000 $\times$ *g*, 10 min) every 72 to 96 h, the wet weight of the resulting cell pellet was determined, and the cells were resuspended in fresh $BG11_0$ to a total volume of 100 ml. A conventional culture was grown in parallel without medium exchange. After 17 days of cultivation, the conventional culture was split, and one-half was pelleted, resuspended in 4-day-old filter-sterilized (0.22-μm pore size) growth medium from the high-density culture, and grown under conventional conditions. After 24 days, cell pellets and growth medium of all three cultures were harvested and further processed for RT-PCR and HPLC analysis.

RNA isolation and RT-PCR. Cells with a wet weight of approximately 0.5 g were pelleted; RNA was isolated by using the hot-TRIzol method (Life Technologies GmbH, Darmstadt, Germany), and supernatants were purified with an RNeasy kit, including on-column DNase digestion (Qiagen, Hilden, Germany). First-strand reverse transcription was carried out using Maxima reverse transcriptase with random oligonucleotides (Thermo Fisher Scientific). For RT-PCR, a LightCycler 480 (Roche Applied Science,

Mannheim, Germany) in combination with a Sybr green-based detection system (SensiFAST SYBR Lo-ROX kit; Bioline, Luckenwalde, Germany) was used. Specific primer pairs for each BGC were designed (Table 2). The RNase P encoding gene *rnpB* was used as a housekeeping gene for standardization, as described previously (11). All primers were tested in PCRs prior to RT-PCR. Each reaction was carried out in four technical replicates. Raw data were converted using the software LC480Converter; subsequent processing and calculation according to the Pfaffl method were carried using LinRegPCR software (27).

Reporter gene cloning and fluorescence microscopy. The 5′ UTR of Npun_F2460 (P-*aptA*) was PCR amplified by using the primers 5′-GAGCTCTTCACTGTTACATTCGGTGACAT-3′ and 5′-CATATGAAATTTGC TACAGAAAGTG-3′, introducing sites for SacI and NdeI, respectively (underlined). The *cfp* coding sequence was amplified from the pECFP-C1 vector (Clontech Laboratories, Mountain View, CA) by using the primers 5′-CATATGGTGAGCAAGGGCGAGGAGCTG-3′ and 5′-GGATCCTTACTTGTACAGCTCGTCCATGCC-3′, introducing NdeI and BamHI sites. The *cfp* fragment was ligated into the cloning vector pDrive (Qiagen); both this construct and the P-*aptA* fragment were digested with SacI and NdeI and ligated. The resulting P-*aptA-cfp* fusion fragment was ligated into the self-replicating vector pRL1049 (28) using SacI and BamHI. The final construct was transferred into *N. punctiforme* PCC 73102 by electroporation, and transformants were generated and verified as described previously (11). Fluorescence microscopy was performed with a confocal laser scanning microscope (LSM 710; Carl Zeiss, Jena, Germany). Images were recorded with filter presets for chlorophyll *a* and enhanced CFP (eCFP). For device control, image acquisition and processing the ZEN software were used. Care was taken to keep all image recording parameters constant for all samples.

General analytical procedures. For HPLC analysis, cell pellets with a wet weight of ~0.3 g were extracted three times by methanol (MeOH) resuspension, sonication for 10 min (Bandelin Sonopuls HD3100; 2-s/2-s pulse/recovery interval), and centrifugation (3,000 × *g*, 4°C, 10 min). Cell-free culture supernatants were loaded onto SepPak Plus C_{18} columns (Waters), and matrix-bound metabolites were washed with 5% (vol/vol) methanol and eluted with methanol. The methanolic extracts were vacuum dried, the resulting pellets were dissolved in 60% (vol/vol) methanol, the debris was removed by centrifugation and filtration (Acrodisc, 0.45-μm pore size; Pall), and samples were subjected to HPLC analysis. HPLC was conducted on a Shimadzu HPLC unit consisting of a system controller SCL-10AVP, a pump LC-10Ai, an autosampler SIL-10A, a fraction collector FRC-10A, and a photo diode array detector (SPD-M-10AVP). Separation was carried out on a SymmetryShield RP18 column (Waters) with a particle size of 3.5 μm, an inner diameter of 4.6 mm, a length of 100 mm, and a precolumn (3.9 by 20 mm) with an identical sorbent. Elution profiles were monitored at 199 nm. Using solvent A as the dilutant for solvent B, the following gradient system was used at a flow rate of 1.0 ml min^{-1}: a 1-min equilibration with 20% solvent B, followed by a linear gradient to 60% solvent B within 35 min, followed by a linear gradient to 100% solvent B in 1 min, and finally back to 20% solvent B within 3 min (solvent A: 0.05% trifluoroacetic acid [TFA] in H_2O; solvent B: acetonitrile, 0.05% TFA). The same solvent routine was used for peak sampling prior to MALDI-TOF analysis.

Prior to MALDI-TOF measurement, sampled HPLC peak fractions were vacuum dried and resuspended in 10 μl of 20% acetonitrile–0.05% TFA. A 0.3-μl portion of the sample solution was mixed with an equal volume of an α-cyano-4-hydroxycinnamic acid matrix (3 mg/ml in 84% acetonitrile,13% ethanol, 3% water, and 0.1% TFA), spotted, and analyzed with a Bruker Microflex LRF apparatus (λ = 337-nm nitrogen laser) in positive-ion reflectron mode. Data were analyzed using the mMass software tool.

NMR spectra were collected using a Bruker Avance 600-MHz spectrometer with a cryoprobe in deuterated dimethyl sulfoxide (DMSO-d_6). Spectra were referenced to the residual solvent peak. UV spectra were obtained on a Shimadzu UV-1800 spectrometer. LC-HRMS measurements were carried out on a Thermo Fisher Scientific Exactive Orbitrap with an electrospray ion source using a Betasil 100-3 C_{18} column (150 by 2.1 mm) and a gradient system: solvent C (H_2O containing 0.1% HCOOH), solvent D (acetonitrile), 5% solvent D for 1 min to 98% solvent D in 15 min, and 98% solvent D for 3 min (flow rate, 0.2 ml min^{-1}).

Sequencing of *Nostoc* sp. strain KVJ2-enriched metagenomic DNA, assembly, and analyses. DNA isolation was performed according to a published protocol with the modifications suggested by the Meeks group (http://microbiology.ucdavis.edu/meeks/xpro5.htm). Purified DNA was analyzed using a Qubit fluorometer (Thermo Fisher), together with a Qubit dsDNA high-sensitivity kit for accurate DNA concentration measurements. A Nextera DNA Library Prep kit was used to generate the sequencing library. A bioanalyzer (Agilent Technologies) was used together with an Agilent high-sensitivity DNA kit for fragment size assessment prior to sequencing. The library was sequenced on a MiSeq machine (Illumina) in Tromsø, Norway, using an MiSeq reagent kit (V3, 2 × 300 bp). The resulting reads were quality checked using FastQC. A draft *de novo* assembly was created using the MIRA 4.0.2 software (29) with default settings. In total, the resulting 3,732 contigs of >500 nucleotides contained 25.3 Mb. Approximately one-third of the contigs belonged to *Nostoc* spp. as analyzed using the PhyloPhytiaS web server (30), and the longest contig contained 344,290 bases. The contigs were compiled into a local nucleotide database file in order to perform similarity searches using BLAST (31). The protein sequences of anabaenopeptin BGC of *N. punctiforme* PCC 73102 (accession numbers ACC81021 to ACC81024) were used as queries to identify the corresponding genes in *Nostoc* sp. KVJ2.

Extraction and isolation of anabaenopeptins from *Nostoc* sp. KVJ2. Freeze-dried algal cells (6.0 g from 1 liter of culture) were resuspended in 80% aqueous methanol (methanol, 300 ml) and extracted by a homogenizer, followed by a sonicator (Bandelin Sonoplus HD2200). After centrifugation at 8,000 × *g* for 10 min, the supernatant was concentrated *in vacuo*. The remaining debris pellets were subjected to two more rounds of extraction, sonication, and centrifugation using 80% aqueous MeOH first and finally 100% MeOH. Vacuum-dried residue was extracted using diethyl ether and H_2O. The aqueous layer

was concentrated and then extracted with *n*-butanol. The *n*-butanol layer was subjected to octadecyl silica (ODS) chromatography (YMC GEL ODS A 60-S50; 3 by 14 cm) with aqueous MeOH (20, 40, 60, and 80%), MeOH, and CH_2Cl_2. The 60% aqueous MeOH-eluted fraction was subjected to reversed-phase column HPLC (Kromasil 100-5C18, 21 by 250 mm) using a gradient system—solvent E (H_2O containing 0.1% TFA), solvent F (83% aqueous acetonitrile), 20% solvent F for 10 min to 100% solvent F in 40 min, UV detection at 220 nm, and a flow rate of 12 ml min^{-1}—to yield anabaenopeptin KVJ827 (peak 8, 7.0 mg), KVJ841 (peak 9, 2.3 mg), and KVJ811 (peak 10, 0.7 mg).

Anabaenopeptins. Anabaenopeptin KVJ827 is a colorless amorphous powder: HRESIMS (positive), *m/z* 828.4282 $[M+H]^+$ (calculated for $C_{44}H_{58}O_9N_7$, *m/z* 828.4291). Anabaenopeptin KVJ841 is a colorless amorphous powder: HRESIMS (positive), *m/z* 812.4348 $[M+H]^+$ (calculated for $C_{44}H_{58}O_8N_7$, *m/z* 812.4341). Anabaenopeptin KVJ811 is a colorless amorphous powder: HRESIMS (positive), *m/z* 842.4449 $[M+H]^+$ (calculated for $C_{45}H_{60}O_9N_7$, *m/z* 842.4447).

Stereochemistry determination of amino acids by Marfey's and Sanger reagents. Each anabaenopeptin (50 μg) was dissolved in 0.5 ml of 6 M HCl containing 1% phenol (anhydrous hydrazine for ureido bond cleavage) and then heated at 105°C for 16 h. After the solvent was removed by nitrogen gas stream, 100 μl of 1 M $NaHCO_3$ and 50 μl of FDAA solution (10 mg/ml in acetone) were added to the residue. The reaction mixture was incubated at 50°C for 1 h and then quenched by 50 μl of 2 M HCl and diluted with 100 μl of 50% aqueous acetonitrile. The obtained derivatives were subjected to liquid chromatography-mass spectrometry (LC-MS). We also used Bruker HCT Ultra ion trap mass spectrometry (Bruker Daltonics, Bremen, Germany) coupled with an Agilent Technologies 1100 series liquid chromatogram system (Agilent, Waldbronn, Germany) with a reversed-phase HPLC Cosmosil MS 100-5C18 column (Nacalai Tesque; 4.6 by 250 mm, flow rate of 1 ml/min) and a gradient system: solvent G (water containing 0.1% formic acid), solvent H (acetonitrile), and 10% solvent H to 90% solvent H in 30 min (see Fig. S13 to S16 in the supplemental material).

To elucidate either L-*allo*- or L-*iso*-Ile in anabaenopeptin KVJ841, an acid hydrolysate of 100 μg of anabaenopeptin KVJ841 was mixed with 50 μl of 1 M $NaHCO_3$, 50 μl of acetone, and 5 μl of Sanger reagent (1-fluoro-2,4-dinitrobenzene) and then incubated at 50°C for 1 h. After quenching by 25 μl of 2 M HCl, the resulting solution was diluted with 100 μl of 50% aqueous acetonitrile. This derivative was analyzed by LC-MS as described above using a reversed-phase HPLC Nucleosil 120-5 C_{18} column (Macherey-Nagel, Düren, Germany; 4.6 by 250 mm, flow rate of 1 ml/min) with a gradient system using solvent G (water containing 0.1% formic acid), solvent H (acetonitrile), and 50% solvent H for 25 min to 99% solvent H in 10 min (see Fig. S16 in the supplemental material).

Allelopathy assay. Allelopathy assays were carried out as follows. The indicator strain *Nostoc* sp. strain KVS11 was prepared by homogenization in liquid $BG11_0$ using a syringe. A freshly plated indicator lawn on solid $BG11_0$ agar (1.2% agar) was overlaid by a thin layer of semisolid (0.7%) medium; inoculation loop-sized agar blocks of the tester *Nostoc* sp. KVJ2 and 5-mm paper disks soaked with 5 μg of anabaenopeptins KVJ811, KVJ827, and KVJ841 in 100% dimethylformamide (DMF; used volume, 2.5 μl) were placed on the top agar. A paper disk with 2.5 μl of 100% DMF served as a negative control, and a disk with 10 μg of streptomycin served as an antibiotic control. Petri dishes were kept under standard cultivation conditions until visible results were obtained in 2 weeks. All tests were performed in three triplicate.

Accession number(s). The sequence of anabaenopeptin BGC of *Nostoc* sp. KVJ2 was deposited in GenBank under accession number MF196967. The metagenome of *Nostoc* sp. KVJ2 is available under accession number NNBU00000000.1.

SUPPLEMENTAL MATERIAL

Supplemental material for this article may be found at https://doi.org/10.1128/AEM.01510-17.

SUPPLEMENTAL FILE 1, PDF file, 1.0 MB.

ACKNOWLEDGMENTS

We are grateful to K. Hinrichs for technical assistance. We thank H. Heinecke, A. Perner, and T. Kindel for the NMR, Thermo Exactive LC-MS, and MALDI-TOF-MS PSD measurements, respectively.

The study was supported by a grant of the German Research Foundation (Di910/12-1) to E.D. Financial support by the DFG-funded Collaborative Research Centre ChemBioSys (SFB 1127) is gratefully acknowledged.

REFERENCES

1. Dittmann E, Gugger M, Sivonen K, Fewer DP. 2015. Natural product biosynthetic diversity and comparative genomics of the cyanobacteria. Trends Microbiol 23:642–652. https://doi.org/10.1016/j.tim.2015.07.008.
2. Kleigrewe K, Gerwick L, Sherman DH, Gerwick WH. 2016. Unique marine derived cyanobacterial biosynthetic genes for chemical diversity. Nat Prod Rep 33:348–364. https://doi.org/10.1039/C5NP00097A.
3. Niedermeyer TH. 2015. Anti-infective natural products from cyanobacteria. Planta Med 81:1309–1325. https://doi.org/10.1055/s-0035-1546055.
4. Calteau A, Fewer DP, Latifi A, Coursin T, Laurent T, Jokela J, Kerfeld CA, Sivonen K, Piel J, Gugger M. 2014. Phylum-wide comparative genomics unravel the diversity of secondary metabolism in cyanobacteria. BMC Genomics 15:977. https://doi.org/10.1186/1471-2164-15-977.

5. Shih PM, Wu D, Latifi A, Axen SD, Fewer DP, Talla E, Calteau A, Cai F, Tandeau de Marsac N, Rippka R, Herdman M, Sivonen K, Coursin T, Laurent T, Goodwin L, Nolan M, Davenport KW, Han CS, Rubin EM, Eisen JA, Woyke T, Gugger M, Kerfeld CA. 2013. Improving the coverage of the cyanobacterial phylum using diversity-driven genome sequencing. Proc Natl Acad Sci U S A 110:1053–1058. https://doi.org/10.1073/pnas.1217107110.
6. Kehr JC, Gatte Picchi D, Dittmann E. 2011. Natural product biosyntheses in cyanobacteria: a treasure trove of unique enzymes. Beilstein J Org Chem 7:1622–1635. https://doi.org/10.3762/bjoc.7.191.
7. Welker M, Dittmann E, von Dohren H. 2012. Cyanobacteria as a source of natural products. Methods Enzymol 517:23–46. https://doi.org/10.1016/B978-0-12-404634-4.00002-4.
8. Hrouzek P, Tomek P, Lukesova A, Urban J, Voloshko L, Pushparaj B, Ventura S, Lukavsky J, Stys D, Kopecky J. 2011. Cytotoxicity and secondary metabolites production in terrestrial *Nostoc* strains, originating from different climatic/geographic regions and habitats: is their cytotoxicity environmentally dependent? Environ Toxicol 26:345–358. https://doi.org/10.1002/tox.20561.
9. Bähr L, Wüstenberg A, Ehwald R. 2016. Two-tier vessel for photoautotrophic high-density cultures. J Appl Phycol 28:783–793. https://doi.org/10.1007/s10811-015-0614-5.
10. Meeks JC, Elhai J. 2002. Regulation of cellular differentiation in filamentous cyanobacteria in free-living and plant-associated symbiotic growth states. Microbiol Mol Biol Rev 66:94–121. https://doi.org/10.1128/MMBR.66.1.94-121.2002.
11. Liaimer A, Helfrich EJ, Hinrichs K, Guljamow A, Ishida K, Hertweck C, Dittmann E. 2015. Nostopeptolide plays a governing role during cellular differentiation of the symbiotic cyanobacterium *Nostoc punctiforme*. Proc Natl Acad Sci U S A 112:1862–1867. https://doi.org/10.1073/pnas.1419543112.
12. Liaimer A, Jenke-Kodama H, Ishida K, Hinrichs K, Stangeland J, Hertweck C, Dittmann E. 2011. A polyketide interferes with cellular differentiation in the symbiotic cyanobacterium *Nostoc punctiforme*. Environ Microbiol Rep 3:550–558. https://doi.org/10.1111/j.1758-2229.2011.00258.x.
13. Takano E, Chakraburtty R, Nihira T, Yamada Y, Bibb MJ. 2001. A complex role for the gamma-butyrolactone SCB1 in regulating antibiotic production in *Streptomyces coelicolor* A3(2). Mol Microbiol 41:1015–1028. https://doi.org/10.1046/j.1365-2958.2001.02562.x.
14. Sharif DI, Gallon J, Smith CJ, Dudley E. 2008. Quorum sensing in cyanobacteria: *N*-octanoyl-homoserine lactone release and response, by the epilithic colonial cyanobacterium *Gloeothece* PCC6909. ISME J 2:1171–1182. https://doi.org/10.1038/ismej.2008.68.
15. Wood SA, Rueckert A, Hamilton DP, Cary SC, Dietrich DR. 2011. Switching toxin production on and off: intermittent microcystin synthesis in a *Microcystis* bloom. Environ Microbiol Rep 3:118–124. https://doi.org/10.1111/j.1758-2229.2010.00196.x.
16. Long BM, Jones GJ, Orr PT. 2001. Cellular microcystin content in N-limited *Microcystis aeruginosa* can be predicted from growth rate. Appl Environ Microbiol 67:278–283. https://doi.org/10.1128/AEM.67.1.278-283.2001.
17. Blin K, Wolf T, Chevrette MG, Lu X, Schwalen CJ, Kautsar SA, Suarez Duran HG, de Los Santos ELC, Kim HU, Nave M, Dickschat JS, Mitchell DA, Shelest E, Breitling R, Takano E, Lee SY, Weber T, Medema MH. 2017. AntiSMASH 4.0: improvements in chemistry prediction and gene cluster boundary identification. Nucleic Acids Res https://doi.org/10.1093/nar/gkx319.
18. Rouhiainen L, Jokela J, Fewer DP, Urmann M, Sivonen K. 2010. Two alternative starter modules for the nonribosomal biosynthesis of specific anabaenopeptin variants in *Anabaena* (*Cyanobacteria*). Chem Biol 17:265–273. https://doi.org/10.1016/j.chembiol.2010.01.017.
19. Liaimer A, Jensen JB, Dittmann E. 2016. A genetic and chemical perspective on symbiotic recruitment of cyanobacteria of the genus *Nostoc* into the host plant *Blasia pusilla* L. Front Microbiol 7:1693. https://doi.org/10.3389/fmicb.2016.01693.
20. Grach-Pogrebinsky O, Carmeli S. 2008. Three novel anabaenopeptins from the cyanobacterium *Anabaena* sp. Tetrahedron 64:10233–10238. https://doi.org/10.1016/j.tet.2008.08.015.
21. Chiang YM, Chang SL, Oakley BR, Wang CC. 2011. Recent advances in awakening silent biosynthetic gene clusters and linking orphan clusters to natural products in microorganisms. Curr Opin Chem Biol 15:137–143. https://doi.org/10.1016/j.cbpa.2010.10.011.
22. Hertweck C. 2009. Hidden biosynthetic treasures brought to light. Nat Chem Biol 5:450–452. https://doi.org/10.1038/nchembio0709-450.
23. Dodds WK, Gudder DA, Mollenhauer D. 1995. The ecology of *Nostoc*. J Phycol 31:2–18. https://doi.org/10.1111/j.0022-3646.1995.00002.x.
24. Halland N, Bronstrup M, Czech J, Czechtizky W, Evers A, Follmann M, Kohlmann M, Schiell M, Kurz M, Schreuder HA, Kallus C. 2015. Novel small molecule inhibitors of activated thrombin activatable fibrinolysis inhibitor (TAFIa) from natural product anabaenopeptin. J Med Chem 58:4839–4844. https://doi.org/10.1021/jm501840b.
25. Sedmak B, Carmeli S, Elersek T. 2008. "Non-toxic" cyclic peptides induce lysis of cyanobacteria-an effective cell population density control mechanism in cyanobacterial blooms. Microb Ecol 56:201–209. https://doi.org/10.1007/s00248-007-9336-9.
26. Rippka R. 1988. Isolation and purification of cyanobacteria. Methods Enzymol 167:3–27. https://doi.org/10.1016/0076-6879(88)67004-2.
27. Pfaffl MW. 2001. A new mathematical model for relative quantification in real-time RT-PCR. Nucleic Acids Res 29:e45.
28. Black TA, Wolk CP. 1994. Analysis of a Het- mutation in *Anabaena* sp. strain PCC 7120 implicates a secondary metabolite in the regulation of heterocyst spacing. J Bacteriol 176:2282–2292. https://doi.org/10.1128/jb.176.8.2282-2292.1994.
29. Chevreux BW, Suhai S. 1999. Genome sequence assembly using trace signals and additional sequence information. Comput Sci Biol Proc Germ Conf Bioinf 99:45–56.
30. Patil KR, Roune L, McHardy AC. 2012. The PhyloPythiaS web server for taxonomic assignment of metagenome sequences. PLoS One 7:e38581. https://doi.org/10.1371/journal.pone.0038581.
31. Altschul SF, Gish W, Miller W, Myers EW, Lipman DJ. 1990. Basic local alignment search tool. J Mol Biol 215:403–410. https://doi.org/10.1016/S0022-2836(05)80360-2.
32. Rottig M, Medema MH, Blin K, Weber T, Rausch C, Kohlbacher O. 2011. NRPSpredictor2: a web server for predicting NRPS adenylation domain specificity. Nucleic Acids Res 39:W362–W367. https://doi.org/10.1093/nar/gkr323.